Synthesis, Crystal Structure and Antimicrobial Properties of 1-Diphenylmethylpiperazine-1,4-Diium Tetrachloridocuprate

Sonia Mokaddem[a], Nedra Korbi[b], Hadda-Imene Ouzari[b] & Habib Boughzala[a*]

[a]Laboratoire de Matériaux et Cristallochimie, Faculté des Sciences de Tunis, Université de Tunis El Manar, 2092 Manar II Tunis, Tunisia.

[b]LR03ES03, Laboratoire Microorganismes et Biomolécules Actives, Faculté des Sciences de Tunis, Université de Tunis El Manar, 2092 Manar II Tunis, Tunisia.

* habib.boughzala@ipein.rnu.tn, * boughzala@yahoo.com

Abstract

New organic/inorganic hybrid $(C_{17}H_{22}N_2)[CuCl_4]$ was elaborated and studied by single crystal X-ray diffraction. The compound crystallizes in the orthorhombic Pbca space group. The isolated $[CuCl_4]^{2-}$ tetrahedra are slightly distorted building a 0-D anionic framework. The double protonation of the organic cation establish N—H···Cl interactions between organic and inorganic moieties leading to self-organized structure. Infrared, UV-Visible and photoluminescence studies were carried out. The in-vitro antibacterial and antifungal activity of the title salt against several microorganisms were studied. The purity of the material was controlled by Rietveld analysis based on structural investigations and X-ray powder diffraction.

Keywords: Crystal structure, DRX, copper, 1-diphenylmethylpiperazine, hybrid material, infrared spectroscopy, antimicrobial activity, RDA

1. Introduction

Hybrid materials are widely used in various fields [1]. The main application is as semiconductors [2] and luminescent materials [3]. This kind of materials is also seen as antimicrobial compounds [4-7]. Otherwise, copper is known for its biological activity [8]. Mixing copper behavior to the new generation of materials leads to a good candidate of copper halides that arouse great interest in diverse fields in biology as anticancer and antifungal [9]. The study of anti-ferromagnetic complexes of these low dimensional molecular magnetic lattices was widely carried out [10-12]. Copper halides are considerably studied because of the particularity of copper geometry. The choice of the organic cation plays a crucial role in the environment around anion through weak interactions as Van der Waals and hydrogen bonding. In this work, the synthesis and the crystal structure of a new tetrachloridocuprate stabilized by the 1-diphenylmethylpiperazin-1,4-diium organic cation is presented. The antimicrobial activity of the title compound is exposed using the Radial Diffusion Assay (RDA).

2. Synthesis and crystallization

The salt was prepared by reaction of 1-diphenylmethylpiperazine and $Cu(NO_3)_2.3H_2O$ (molar ratio 1:1) in an equal volume water-ethanol (10mL) mixed to 3 mL of hydrochloric acid 37%. The solution was stirred for one hour at 333K. After two weeks, single yellow crystals suitable for X–ray diffraction were grown by slow evaporation at room temperature.

3. X-ray structure determination

A yellow crystal has been selected for X-ray diffraction analysis. Data collection was performed on an Enraf–Nonius CAD-4 diffractometer, operating at 298 K with (Mo K$_\alpha$ radiation, λ= 0.71069Å). CAD4-Express program [13] was used to integrate the reflection intensities. An empirical ψ-scan absorption correction was applied [14]. The structure has been solved by direct methods using SHELXS-2014 software [15] and refined by least-square full-matrix based on F^2 using SHELXL-2014 software [16]. A summary of the crystallographic data and structural

determination is provided in Table 1. The final reduced atomic coordinates and the equivalent thermal factors are listed in Table 2. The hydrogen atoms were located using the riding model. The program DIAMOND version 3.0 [17] was used for molecular graphics. The complete set of the structural parameters in CIF format is available from the Cambridge Crystallographic Database Centre (CCDC 1852657). A copy can be obtained free of charge from www.ccdc.cam.ac.uk/data_request/cif or deposit@ccdc.edu.

Table 1. Crystallographic data and refinement parameters in the crystal structure of $C_{17}H_{22}N_2CuCl_4$.

Crystal data	
Chemical formula	$C_{17}H_{22}N_2Cu_4Cl4$
Molecular weight (g.mol^{-1})	459.70
Crystal System / Space Group **Space group**	Orthorhombic / P back Pbca
Temperature (K)	298
a. b. c (Å) / V (Å^3)	10.8971 (10). 13.343 (2). 26.909 (3) / 3912.5 (8)
Crystal shape / color **Crystal colour**	Prism / Yellow Yellow
Z	8
D_x (Mg m^{-3})	1.561
μ (mm^{-1})	1.66
Data collection	
Diffractometer	Enraf Nonius CAD4
Absorption correction	ψ scan
Monochromator **Radiation type λ(Å)**	Graphite Mo Kα 0.71073
Measured reflections **Observed reflections** **Independent reflections**	6822 1867 4249
Variation of indices hkl	h = −13 to 5 k = −1 to 17 l = −1 to 34
Refinement	
R[F^2 > 2σ(F^2)] **wR(F^2)** **S**	0.062 0.219 0.98
Parameters	217
Δρ$_{max}$. Δρ$_{min}$ (e Å^{-3})	0.63, −0.50

Table 2. Coordinates and isotropic displacement parameters (Å^2) of atoms in the crystal structure of $C_{17}H_{22}N_2CuCl_4$.

Atome	x	y	z	U_{eq}
Cu	0.40875(9)	0.10530(6)	0.33315(4)	0.04966(32)
Cl1	0.36851(24)	0.00884(18)	0.27651(11)	0.09383(93)
Cl2	0.59822(17)	0.18400(14)	0.30739(7)	0.05089(50)
Cl3	0.45738(21)	0.02133(16)	0.40088(8)	0.06377(61)
Cl4	0.27734(20)	0.22748(16)	0.32567(9)	0.06783(65)
N1	0.28209(48)	0.33515(38)	0.13757(21)	0.03789(136)
H1A	0.21581	0.29178	0.14955	0.045
C1	0.23958(60)	0.38245(51)	0.08882(26)	0.03994(166)
H1	0.30250	0.43127	0.07927	0.048
C2	0.23209(61)	0.30771(53)	0.04761(25)	0.04014(169)
C3	0.30627(71)	0.31910(56)	0.00627(27)	0.04926(188)
H3	0.36242	0.37155	0.00534	0.059
C4	0.29899(81)	0.25591(68)	-0.03269(31)	0.06274(229)
H4	0.35019	0.26511	-0.05996	0.075
C5	0.21652(77)	0.17800(64)	-0.03245(30)	0.05641(222)
H5	0.21127	0.13517	-0.05964	0.068
C6	0.14210(68)	0.16360(57)	0.00793(31)	0.05382(205)
H6	0.08699	0.11039	0.00851	0.065
C7	0.14931(69)	0.22815(57)	0.04753(30)	0.05105(194)
H7	0.09809	0.21861	0.07477	0.061
C8	0.12113(58)	0.43967(47)	0.09416(24)	0.03575(159)
C9	0.10524(68)	0.51809(52)	0.06072(26)	0.04460(175)
H9	0.16863	0.53556	0.03926	0.054
C10	-0.00372(82)	0.56987(54)	0.05925(34)	0.05713(225)
H10	-0.01391	0.62174	0.03653	0.069
C11	-0.09565(81)	0.54611(57)	0.09037(32)	0.05930(217)
H11	-0.16876	0.58196	0.08902	0.071
C12	-0.08311(69)	0.46915(61)	0.12438(30)	0.05607(202)
H12	-0.14671	0.45312	0.14601	0.067
C13	0.02566(67)	0.41680(53)	0.12549(28)	0.04761(189)
H13	0.03477	0.36454	0.14806	0.058
C14	0.39384(62)	0.27050(52)	0.12983(28)	0.04491(166)
H14A	0.37447	0.21804	0.10614	0.054
H14B	0.45920	0.31100	0.11585	0.054
C15	0.43712(75)	0.22432(61)	0.17658(30)	0.05827(220)
H15A	0.51219	0.18748	0.17015	0.07
H15B	0.37601	0.17702	0.18829	0.07
C16	0.35190(71)	0.36592(62)	0.22416(26)	0.05277(195)
H16A	0.37305	0.41916	0.24716	0.064
H16B	0.28650	0.32668	0.23897	0.064
N2	0.46057(57)	0.30092(46)	0.21630(23)	0.05303(165)
H2A	0.47914	0.26992	0.24460	0.064
H2B	0.52446	0.33862	0.20764	0.064
C17	0.30754(66)	0.41064(51)	0.17692(23)	0.04143(170)
H17A	0.36871	0.45741	0.16476	0.05
H17B	0.23306	0.44818	0.18350	0.05

Table 3. Characteristic of the hydrogen bonds in the crystal structure of $C_{17}H_{22}N_2CuCl_4$.

D—H···A	D—H	H···A	D···A	D—H···A
N1—H1A···Cl3[i]	0.980	2.249	3.206(6)	165.32
N2—H2C···Cl3	0.890	2.420	3.271(6)	160.25
N2—H2D···Cl1[ii]	0.890	2.385	3.154(6)	144.84

Symmetry codes : (i) x-1/2, y, -z+1/2 ; (ii) x-1, y+1/2, -z+1/2.

Table 4. Selected bond lengths (Å) and angles (°) in the crystal structure of $C_{17}H_{22}N_2CuCl_4$.

Cu—Cl1	2.199 (2)	C8—C13	1.373 (9)
Cu—Cl2	2.418 (2)	C8—C9	1.393 (9)
Cu—Cl3	2.204 (2)	C8—C1	1.507 (9)
Cu—Cl4	2.179 (2)	C9—C10	1.371 (10)
N1—C1	1.526 (8)	C2—C3	1.386 (9)
N1—C14	1.505 (8)	C10—C11	1.346 (11)
N1—C17	1.488 (8)	C2—C7	1.392 (10)
C2—C1	1.493 (9)	C6—C7	1.372 (10)
C3—C4	1.347 (10)	C12—C13	1.377 (10)
C4—C5	1.371 (11)	C14—C15	1.479 (10)
C5—C6	1.373 (10)		
Cl4—Cu—Cl1	108.85 (10)	C7—C6—C5	119.6 (7)
Cl4—Cu—Cl3	127.92 (9)	C2—C1—C8	111.2 (5)
Cl1—Cu—Cl3	105.61 (10)	C2—C1—N1	112.2 (5)
Cl4—Cu—Cl2	102.13 (8)	C8—C13—C12	121.7 (7)
Cl1—Cu—Cl2	105.80 (10)	C8—C1—N1	112.8 (5)
Cl3—Cu—Cl2	104.62 (8)	C15—C14—N1	112.4 (6)
C17—N1—C14	109.7 (5)	C14—C15—N2	111.9 (6)
C17—N1—C1	112.8 (5)	C16—C17—N1	113.3 (6)
C14—N1—C1	111.4 (5)	N2—C16—C17	111.9 (6)
C3—C2—C7	117.3 (7)	C16—N2—C15	111.3 (5)
C3—C2—C1	119.4 (6)	C9—C8—C1	115.3 (6)
C7—C2—C1	123.2 (6)	C10—C9—C8	120.2 (7)
C4—C3—C2	121.4 (7)	C11—C10—C9	120.8 (7)
C3—C4—C5	120.7 (8)	C10—C11—C12	120.6 (7)
C4—C5—C6	119.7 (7)	C13—C8—C9	118.0 (6)
C6—C7—C2	121.2 (7)	C13—C12—C11	118.7 (7)

4. Structural description

The asymmetric unit of the crystal structure, represented in Figure 1, is built up by one tetrahedron $[CuCl_4]^{2-}$ and one organic cation from diphenylmethylpiperazine doubly protonated.

Several geometries can be adopted when using copper coordinated to halogens anions. Including tetrahedral, square pyramidal, square planar and square-bipyramidal [19, 20] we can also find copper in octahedral geometry. This diversity allows copper halides to be a good candidate in the class of self-organized organic-inorganic hybrid compounds [12].

As shown in Figure 2, the environment around the anion can be described by a tetrahedron of $[CuCl_4]^{2-}$ surrounded by three organic ligands of diphenylmethylpiperazine linked through hydrogen bonds. The double protonation of the diphenylmethylpiperazine establish bridges between $[CuCl_4]^{2-}$ and the organic moieties. In agreement with the angular values of the copper-chlorine bonds summarized in the table 3, the tetrahedral copper coordination presents a slight distortion plausibly due to the hydrogen bridges N—H...Cl and particularly the result of the Jahn Teller effect.

As represented in the Figure 3, the cationic environment is revealing the protonation of organic moiety involving the couple of nitrogen's of diphenylmethylpiperazine in hydrogen bonding with Cl1 and Cl3 vertices. Each cation of $(C_{17}H_{22}N_2)^{2+}$ is linked to three tetrahedra of $[CuCl_4]^{2-}$. The $(C_{17}H_{22}N_2)^{2+}$ cation adopts a chair conformation for piperazinium and a quite planar conformation for the two cycles of phenyl characterized by a slight r.m.s deviation 0.0028(4)Å for the first cycle the maximum deviations are for C9 and -0.004(6) Å for C8. The second cycle represents almost the same r.m.s deviation with 0.004(5) Å for C17 and -0.003(6) Å for C16 as maximum deviations.

The organic chains are spread along the c axis forming parallel waved chains running along the b direction. The Figure 4, reveals that these chains are arranged parallel to a twofold screw axis parallel to a direction alternated with $[CuCl_4]^{2-}$ tetrahedra. The isolated $[CuCl_4]^{2-}$ tetrahedra classes this compound among the 0-D hybrid materials.

Along the b direction (Figure 5), the steric hindrance avoid the presence of voids in this structure even so, we can see that the shape of the organic moieties prohibits to inorganic tetrahedra to be spread away. The shape of organic moieties suggests that we can lodge small entities that may bring new behavior to this material.

In fact, hydrogen bonding and (π-π) stacking are the most important links in metal halides ensuring cohesion and stabilizing the crystal packing through bridges built between the organic and inorganic subnetworks.

For organic molecules an infrequent (π-π) mode of stacking is observed. In fact these interactions are essential for building framework and impacting on properties of metal halide materials. In the title salt, the anionic environment can be described by $[CuCl_4]^{2-}$ tetrahedron linked to three organic cations of 1-diphenylmethylpiperazine-1.4-diium via Cl1 and Cl3 vertices as N1—H1A···Cl3[i], N2—H2C···Cl3 and N2—H2D···Cl1[ii].

Cationic environment is made up by one molecule of 1-dimethylphenylpiperazine-1.4-diium surrounded by three $[CuCl_4]^{2-}$ tetrahedra. The organic molecules are connected through (π-π) stacking by edge-to- face mode. The centroïd distance Cg1...Cg2 is about 4.674(1) Å calculated for the two phenylic cycles in the same cation and around 4.954(1) Å measured for two independent cations.
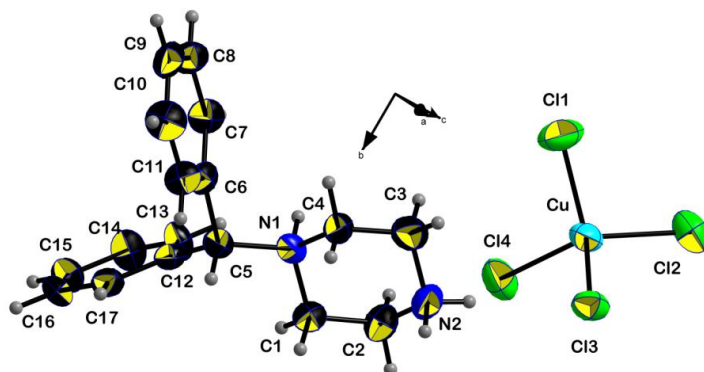
Figure 1: ORTEP of the asymmetric unit in the crystal structure of $C_{17}H_{22}N_2CuCl_4$. Displacement ellipsoids at drawn with 50% probability level.
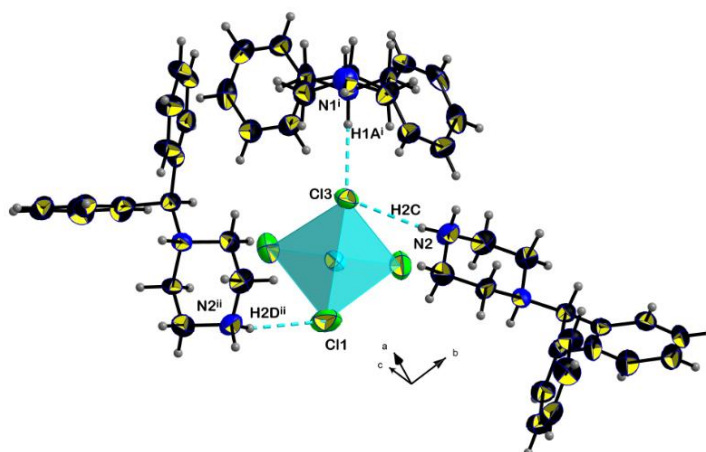

Figure 2. The hydrogen interaction around $[CuCl_4]^{2-}$ in the crystal structure of $C_{17}H_{22}N_2CuCl_4$ shown as dashed lines. Displacement ellipsoids are displayed at the 50% probability level. Symmetry codes : (i) −x, y−1/2, −z+1/2; (ii) −x+1/2, y−1/2, z.
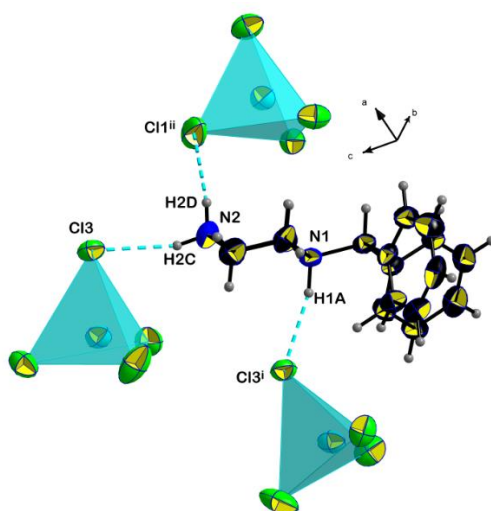

Figure 3: The environment around the $(C_{17}H_{22}N_2)^{2+}$ cation showing hydrogen bridging in the crystal structure of $C_{17}H_{22}N_2CuCl_4$. Symmetry codes : (i) −x, y−1/2, −z+1/2; (ii) −x+1/2, y−1/2, z.
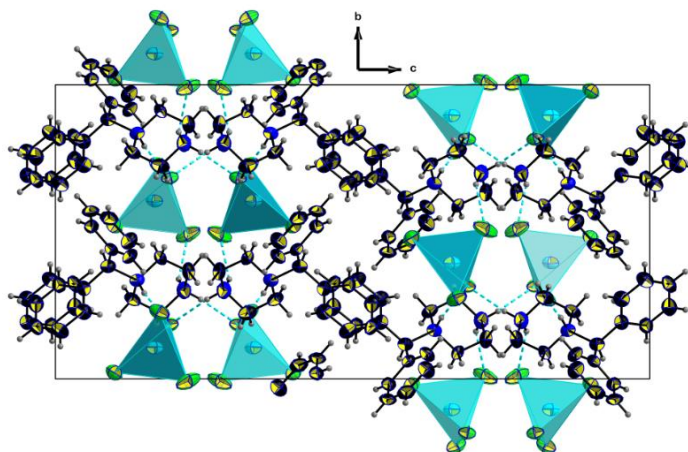
Figure 4: Self organized assembly system in the crystal structure of $C_{17}H_{22}N_2CuCl_4$ showing the alternate arrangement of organic-inorganic sheets.
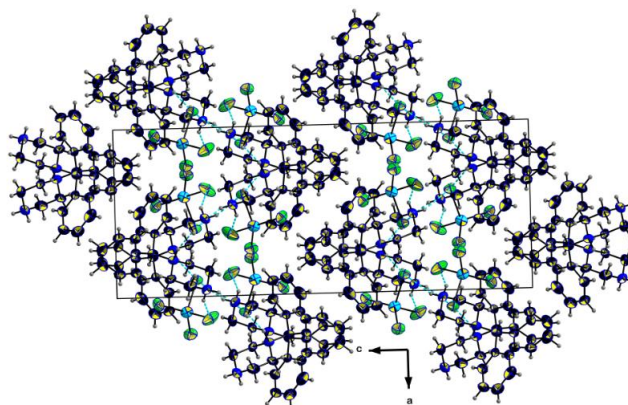
Figure 5: Steric hindrance of organic cations in the crystal structure of $C_{17}H_{22}N_2CuCl_4$.

5. Spectroscopic study

Trying to explore the vibrational and the electronic transitional activities in the studied structure, three spectroscopic experimental investigations were carried out, the InfraRed (IR), the UV-visible and the Photoluminescence (PL). In addition, theoretical calculations were performed using the program CaChe [22], to identify the High Occupied Molecular Orbital and the Low Unoccupied Molecular Orbital (HOMO-LUMO) orbital's energy and evaluate the HOMO-LUMO gap.

5.1. Infrared spectroscopy

The infrared (IR) absorption frequencies of the compound $C_{17}H_{22}N_2CuCl_4$ were studied using the FT–IR Bruker Tensor 27 spectrophotometer in the range of 1400-400 cm^{-1} wavenumber containing the most significant solid state absorption bands. The sample was ground with 98% weight KBr and pressed into 1cm diameter discs. Calculated IR spectrum was realized using PM3 FORCE method implemented in the CAChe program [22]. Compared to the observed spectrum the calculated one exhibits a shift towards the high frequencies which can be explained by the choice of the computational method using the PM3 FORCE in our case did not rigorously apply the effect of the electronic correlation. This semi-empirical calculation method assumes that the molecules are isolated when they are actually involved in hydrogen bonds or in other electronic interactions. The calculated and observed IR spectra of this compound are presented in Figure 6a and 6b respectively.

Table 5. Observed and calculated vibration frequencies (cm^{-1}) in the crystal structure of $C_{17}H_{22}N_2CuCl_4$ with proposed assignments.

Observed	calculated	Assignments
752	800	δ_{c-N-c}
1385	1500	ν_{C-N}
1623	1800	$\nu_{C=C}/\delta_{N-H}$
3127	-	ν_{C-H}
3650	3500	ν_{N-H}
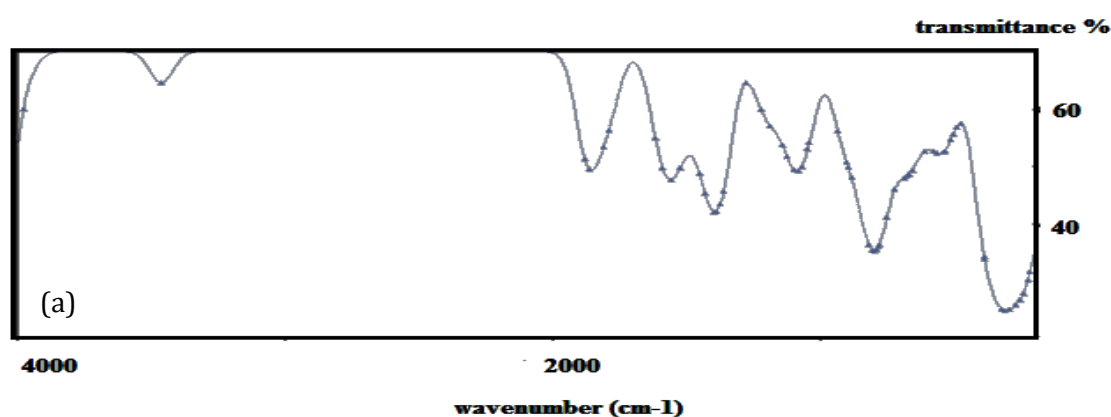
Figure 6. (a) Calculated and (b) Observed Infrared spectra of the crystal structure of $C_{17}H_{22}N_2CuCl_4$.
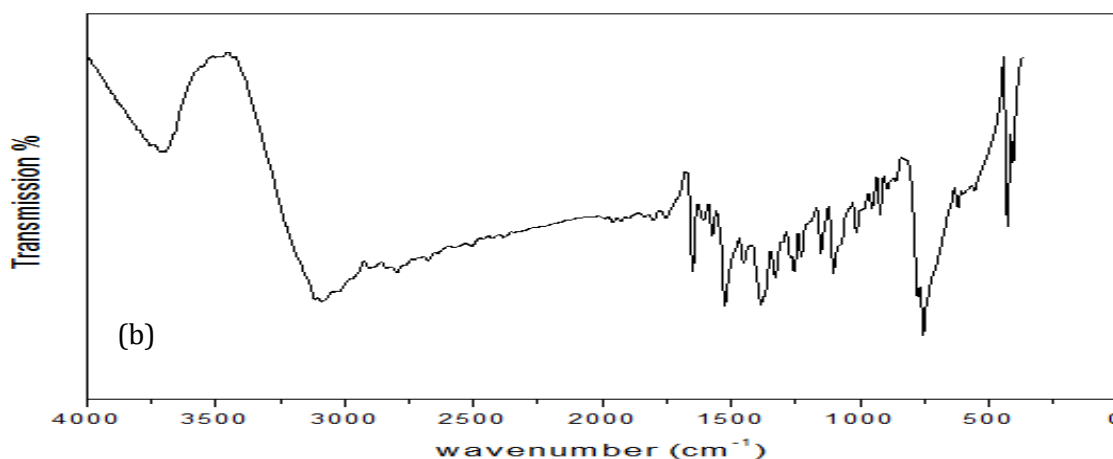
5.2. UV-visible

Using a Perkin Elmer lambda950 spectrophotometer scanning the UV-visible spectral domain, the crystalline sample was ground in an agate mortar. A pinch of the compound was added to a water drop and kept to dry at room temperature for several minutes. The absorbance registered spectrum represented in Figure 7. exhibits three particular wavelengths 321, 455 and 782 nm assigned respectively to the transition π-π* of the organic cation $(C_{17}H_{22}N_2)^{2+}$, the ligand-metal charge transfer (LMCT) and to the d-d copper transition of the anionic inorganic cluster $CuCl_4$.
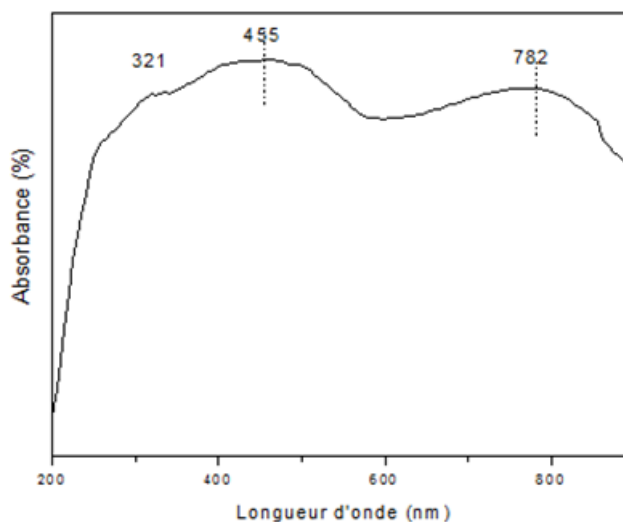
Figure 7. UV-Visible absorption spectrum of $C_{17}H_{22}N_2CuCl_4$.

5.3. Photoluminescence

Using a Perkin-Elmer LS 55 luminescent spectrophotometer equipped with a 250nm exciting luminous radiation, the crystalline sample was like for the UV-visible experiment.

The emission spectrum of the studied compound represented in Figure 8. reveals three bands elucidated after a deconvolution realised by the program Origin 9.0 [24] using a Gaussian profile without considering any background. The first one (red) centred on 380 nm related to the d-d copper transition [25-26]. The second one (green) with 487 nm can be attributed to the organic cation emission [27]. The last and most intense one (533 nm) can be assigned to an electronic transition.
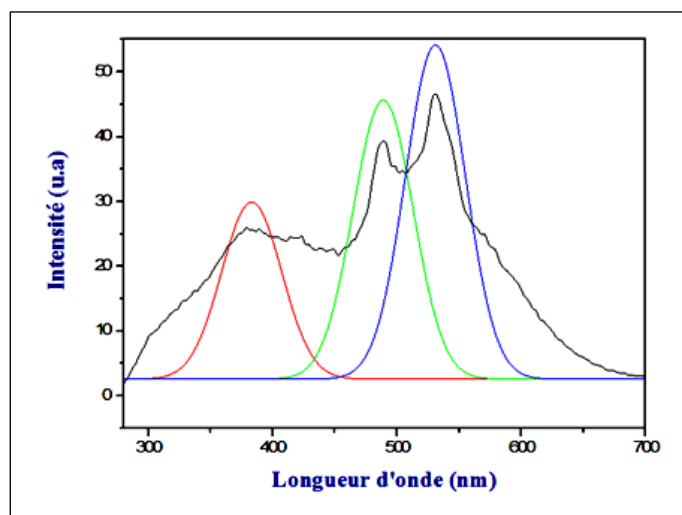

Figure 8. Photoluminescent emission spectrum of $C_{17}H_{22}N_2CuCl_4$.

5.4. HOMO-LUMO gap calculation

The Discrete Fourier Transform DFT's calculations were carried out by the program CaChe [22] using the semi-empirical Parameterized Model number 3 (PM3) for the title compound. The graphical representation calculated on Figure 9 is showing the orbitals frontiers in $C_{17}H_{22}N_2CuCl_4$. Located on the inorganic moiety, the HOMO exhibits the highest contribution compared to the LOMO identified on the organic cation. The gap deduced from the simulation is 1,373 eV. The studied material can be ranged among the copper based semiconductors hybrids.
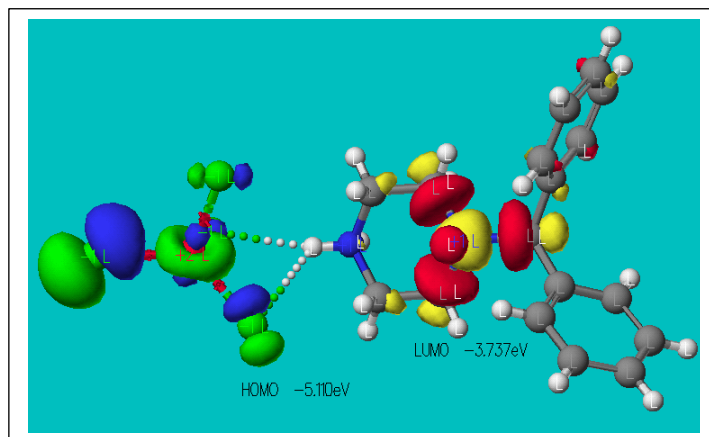

Figure 9. Photoluminescent emission spectrum of $C_{17}H_{22}N_2CuCl_4$.

6. Analysis of DPMPD-TCC antimicrobial activity

The antimicrobial activity of the 1-diphenylmethylpiperazine-1, 4-diium tetrachloridocuprate DPMPD-TCC salt was determined using the Radial Diffusion Assay (RDA)[18] toward different Gram negative (*Salmonella enterica* and *Shigella flexneri*) and Gram positive (*Enterococcus feacalis*, *Staphylococcus aureus* and *Bacillus cereus*) bacteria, as well as, Human pathogenic fungi of Candida (*C. albicans*, *C. parapsilosis* and *C. sakei*). Sabouraud agar and Tryptic Soya Agar media were used for the growth of fungi and bacteria respectively.

Minimal inhibitory concentration (MIC), which corresponds to the lowest concentration exhibiting microbial growth inhibition, was evaluated by the same method using different concentration of the compound. .

The bioactive compound $C_{17}H_{22}N_2CuCl_4$ exhibited growth inhibition only toward Gram positive bacteria. *Enteroccocus fecalis* was found to be the most sensitive strain with an inhibition zone diameter of 12mm and a MIC of 0.2 mg/ml. While the MIC of *Staphylococcus aureus* and *Bacillus cereus* was 0.5 mg/ml (Table 6).

Table 6. Diameter of inhibition and minimal inhibitory concentration (MIC) of organisms for $(C_{17}H_{22}N_2).[CuCl_4]$.

Organism	Diameter of	Minimal inhibitory
Candida albicans	0	-
Candida parapsilosis	0	-
Candida sake	7	0,2
Enteroccocus fecalis	12	0,2
Bacillus cereus	8	0,5
Staphylococcus aureus	8	0,2
Salmonella enterica	0	-
Shigella flexneri	0	-

* The mentioned diameter of the growth inhibition zones corresponds to a concentration of 1mg/ml of the compound.

The absence of inhibitory effect recorded against Gram negative bacteria may be explained by the presence of the outer membrane in the bacterial cell wall of Gram negative bacteria acting as a barrier for some antibiotics and other compounds and giving them a particular rigidity [21]

As for the human pathogenic fungi the best inhibitory activity was observed for *C. sake* (8mm), with a MIC of 0.2mg/ml, followed by *C. albicans* and *C. parapsilosis* with a growth inhibition zones of 6 and 4mm respectively (Figure 10)
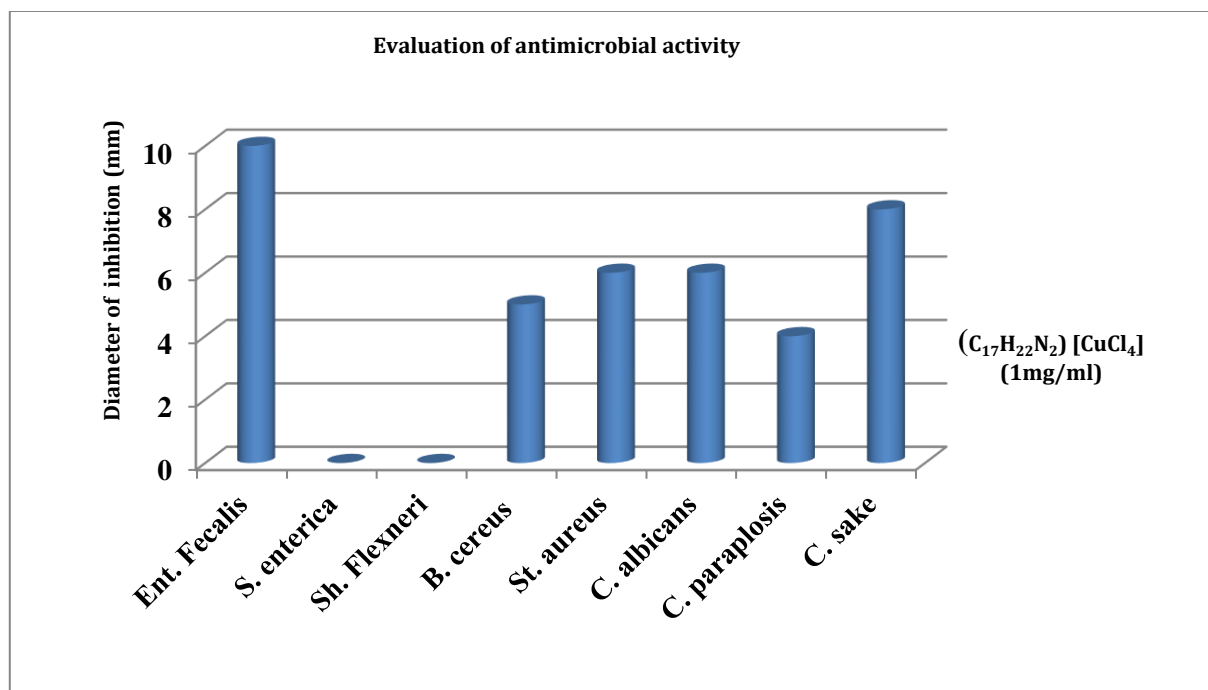

Figure 10: Antimicrobial activity of $C_{17}H_{22}N_2CuCl_4$ (1mg/ml).

7. X-ray powder diffraction

Trying to know if the chemical synthesis is leading to pure sample the X-ray powder diffraction (XRPD) experiment was carried out using a D8 ADVANCE Bruker diffractometer equipped with Bragg-Brintano geometry and Lynxeye accelerator using $Cu(K\alpha_1/\alpha_2 = 1.54060/1.54439$ Å) wavelength with step-scanning ($\Delta 2\theta = 0.02°$), a constant time interval of 0.018 s and 2θ scanning range of [5-70] °.

Based on the structural data and the observed powder diffraction pattern the Rietveld study was performed using TOPAS 4.2. [23]. The calculated raw diffraction is compared to the observed one using the curve difference. The study reveals a high purity of the sample since all the Bragg pics are indexed by the crystallographic data of the studied compound confirmed by the reliability factors and the χ^2 value visible on Figure 11. Thus, the observed physical behavior of the sample can be attributed to the studied structure of $C_{17}H_{22}N_2CuCl_4$. Nevertheless, a consistent amorphous fraction is noted in the mixture by the presence of a diffuse and very large reflection centered around 14°. The thin and sharp observed reflections proof the high crystallinity of the compound.
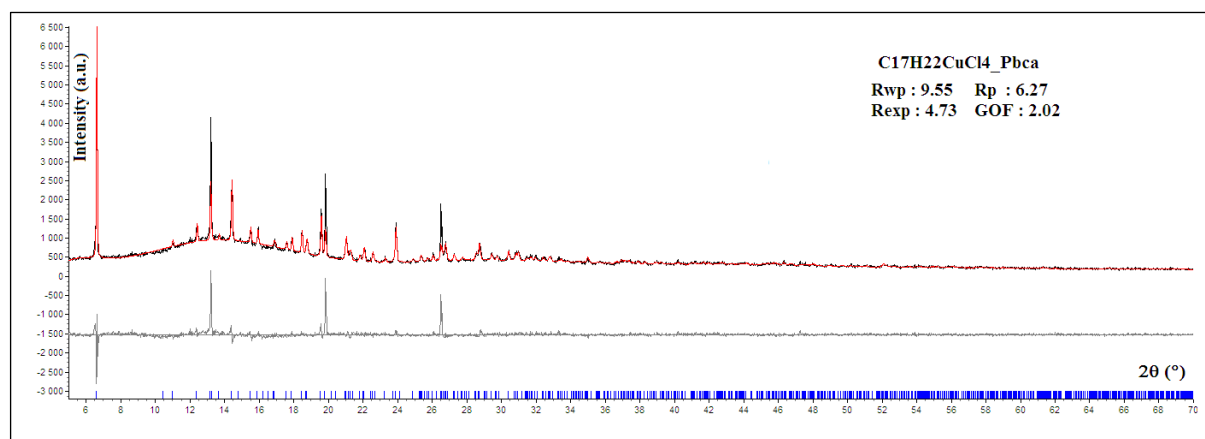
Figure 11: Summary of the Rietveld study carried out on the compound $C_{17}H_{22}N_2CuCl_4$.

4. Conclusion

A new salt around copper was synthesized and grown by slow evaporation. The title salt crystallizes in the orthorhombic Pbca space group. The X-ray diffraction study reveals a 0-D hybrid structure self-organized in alternating sheets of organic and inorganic moieties linked through hydrogen interactions ensuring the crystal packing cohesion. The anionic moiety $[CuCl_4]^{2-}$ is surrounded by three organic cations $(C_{17}H_{22}N_2)^{2+}$ through hydrogen bridging and (π-π) stacking. Spectroscopic investigations combined to the PM3 semi-empirical simulation facilitate the assignment of the observed IR absorption bands to the vibration frequencies, the interpretation of the UV-Visible spectrum and the photoluminescence emission. The antimicrobial study results show that the salt acts only against gram positive bacteria and for antifungal. The best result was observed for the human pathogenic fungi *candida sake*. The Rietveld refinements confirm the sample purity and allow the attribution of the observed behavior of the sample to the solved and refined crystal structure.

References

1. Rao, C. N. R.; Chheetham, A. K; Thirumurugan, A. J. Phys. Condens. Mater. 2008, 20, 1-23.

    Fang, Q. R.; Zhu, G. S.; Jin, Z.; Xue, M. ; Wei, X. ; Wang D. J.; Qiu S. L. Angew. Chem. Inter. Edn. 2006, 45, 6126-6130.

2. Wang, S.; Hou, Y.; Wang, E.; Li, Y.; Xu, L.; Peng, J.; Liua S.; Hua, C. New J. Chem. 2003, 27, 1144-1147.

3. Gust, R.; Beck, W.; Jaouen, G.; Schoenenberger, H. Coord. Chem. Rev. 2009, 253, 2760-2779.

4. Gust, R.; Beck, W.; Jaouen, G.; Schoenenberger, H. Coord. Chem. Rev. 2009, 253, 2742-2759.

5. Boulikas, T.; Pantos, A.; Bellis E.; Christofis, P. Cancer Ther. 2007, 5, 537-537.

6. Zutphen, V.; Reedijk, S. J. Coord. Chem. Rev. 2005, 249, 2845-2845.

7. Solomon, E. I.; Hepper, D. E.; Johnston, E. M.; Ginsbach, J. W.; Cirera J.; Qayyum, M.; Kieber-Emmons, M. T.; Kjaergaard, C. H.; Hadt, R. G.; Tian, L. Bioinorganic Enzymology. 2014, 114, 3659-3853.

8. Creaven, B.; Duff, B.; Egan, D.;Kavanagh, K.; Rosair, G.; Thangella, V.; Walsh, M. Inorg. Chim. Acta. 2010, 363, 4048–4058.

9. Hammar, P.; Dender, D.; Reich, D. J. Appl. Phys. 1997, 81, 4615-4617.

10.   Shapiro, A.; Landee, C.; Turnbull, M.; Jornet, J.; Deumal, M.; Novoa, J.; Robb, M.; Lewis, W. J. Am. Chem. Soc. 2007, 129, 952-959.

11.   Dammak, T., Boughzala, H.; Mlayah, A.; Abid, Y. J. Lumin. 2016, 173, 213–217.

12.   Harms, K; Wocadlo, S. *XCAD4*. Program for Processing CAD-4 Diffractometer Data. (1995), University of Marburg, Germany.

13.   North, A.C.T.; Phillips, D.C.; Mathews, F. S. Acta Cryst. A 1968, 24,351–359.

14.   Sheldrick, G. M. *Acta Cryst*. *A* 2008, 64, 112-122.

15.   Sheldrick, G. M. *Acta Cryst*. *C* 2015, 71, 3–8.

16.   Brandenburg, K. DIAMOND. 3.1, Crystal Impact GbR, Bonn, Germany, 2008.

17.   Lehrer, RI. ; Rosenman, M., ; Harwig, SS., Jackson, R., Eisenhauer, P. Ultrasensitive assays for endogenous antimicrobial polypeptides. J immunological methods. (1991),137,167-73.

18.   Bhattacharya, R.; Chanda, S.; Bocelli, G.; Cantoni, A.; Ghosh, A. J. Chem. Cryst. 2004, 34, 393-400.

19.   Yuan, B. L.; Lan, H.C. ; Chen, Y.P. ; Li, Y.B. Acta Cryst. E 2004, 60, 617–619.

20.   Walsh, S. E. ; Maillard, J. Y. ; Russell, A. D. ; Catrenich, C. E. ; Charbonneau, D. L. ; Bartolo, R. G. J Hospital Infection, (2003), 55, , 98-107.

21.   CaChe: work system Pro Version 7.5.0.85, Fujitsu Limited.2000–2006 Oxford Molecular.

22.   Coelho, A. A. TOPAS, version 4.2 (Computer Software), Coelho Software, 2009.

23.   Origin 9.0. OriginLab Corporation One Roundhouse Plaza Northampton, MA 01060. USA

24.   C.Tamuly, N. Barooah, A. S. Batsanov,R. Kataky et J. B. Baruah, Inorg. Chem. Comm., 8, (2005), 689–691

25.   T. Dammak, H. Boughzala, A. Mlayah et Y. Abid, J. of Luminescence, 173, (2016), 213-217.

26.   R. Fu, S. Hu, X. Wu, Cryst. Eng. Comm. 13, (2011), 6334–6336.